Bound and Pore Water-Discriminated MRI in Human Cortical Bone

R. Adam Horch[1,2], Jeffry S Nyman[3,4], Daniel F Gochberg[2,5], Mary Kate Manhard[1,2], and Mark D Does[1,2]

[1]*Biomedical Engineering, Vanderbilt University, Nashville, TN, United States,* [2]*Vanderbilt University Institute of Imaging Science, Vanderbilt University, Nashville, TN, United States,* [3]*VA Tennessee Valley Healthcare System,* [4]*Department of Orthopaedics & Rehabilitation, Vanderbilt University, Nashville, TN, United States,* [5]*Radiology and Radiological Sciences, Vanderbilt University, Nashville, TN, United States*

Introduction

Human cortical bone MRI has become clinically feasible with modern ultrashort-echo time (uTE) imaging [1] and related methods. The cortical bone uTE signal consists of predominately collagen-bound water ($T_2 \approx 400$ μs) and pore space water (T_2 = 1ms-1s) [2]. Previously, bound and pore water signal sizes were directly (r^2=0.68) and inversely (r^2=0.61) correlated to mechanical properties of bone, although the net signal was poorly correlated (r^2=0.06) [3]. Thus, bound and pore water likely need to be discriminated for MRI assessment of fracture risk. Off-resonance effects and potentially similar T_2*s may confound a T_2*-based spectroscopic approach for bound/pore water discrimination, although recent work has shown promising results [4]. Herein, we pursue alternative uTE approaches that incorporate T_2-selective adiabatic full passage (AFP) pulses for discriminately imaging bound or pore water. These approaches were previously validated with non-imaging spectroscopy [5], and here we show bound and pore water images collected from human cadaveric femurs in a clinically-compatible manner. By avoiding potentially confounding spectroscopic measurement and analysis, these AFP-based approaches potentially quantify both bound and pore water as important determinants of bone's resistance to fracture.

Methods

Human femur midshafts were obtained from the Vanderbilt Tissue Donor Program. Midshafts were cleaned of surrounding soft tissues but intramedullary marrow was left intact. 3D radial uTE MRI was performed at 4.7T and consisted of 1) a double-AFP uTE sequence (DAFP, Fig 1a), which isolated long-T_2 pore water by saturating short-T_2 bound water via a double-AFP (2 x 10ms/3.5kHz hyperbolic secant AFPs, 50 ms TR, 50 μs TE, 60º hard excitation), and 2) a steady-state AFP inversion recovery uTE sequence (AIR, Fig 1b), which isolated short-T_2 bound water by selectively inverting and then nulling the pore water via appropriate choice of TI (10ms/3.5kHz hyperbolic secant AFP, 300ms TR, 90ms TI, 50 μs TE, 30º hard excitation). Peak B_1 and imaging gradient amplitudes were constrained to clinically-relevant values of 1 kHz and 20 mT/m, respectively. A 150mM $CuSO_4$ phantom ($T_1 \approx 10$ ms) with 10% H_2O and 90% D_2O was placed adjacent to midshafts during imaging for converting bone signals to quantitative units of absolute concentration (mol $^1H/L_{bone}$).

Results and Discussion

Quantitative pore and bound water images were successfully generated with the DAFP and AIR uTE methods. Figure 2 (top) shows complementary axial slices through the femoral midshaft of a 67 y.o. female, as generated by the DAFP and AIR pulse sequences. Quantitative bound and pore water maps, determined from the imaging phantom and AIR/DAFP signal equations, show considerable variation in bound and pore water content (Fig 2, bottom), especially between the posterior (image left) and anterior (image right) sides. Voxel-wise, a reciprocal relationship between bound and pore water content was observed, consistent with previous findings [3]. These images depict the bound and pore water contrast available to clinical imaging via the DAFP and AIR methods, which provides diagnostically-useful information across the cortical bone volume.

References:

1) Techawiboonwong, A., et. al. *Radiology* 48(2008): 824-833.

2) Horch, RA., et. al. *Magn. Reson. Med.* 64(2010): 680–687.

3) Horch, et. al. *PLoS One.* (2011): e16359.

4) Diaz, E., et. al. *NMR Biomed.* (2011): 10.1002/nbm.1728.

5) Horch, RA., et. al. *Proc. 18th ISMRM.* (2011): 1117.

Acknowledgements: The authors would like to acknowledge financial support from the NIH # EB001744, the Vanderbilt Discovery Grant, and the ASEE NDSEG (32 CFR 168a).

Figure 1: Pulse sequences and M_z for DAFP(a) and AIR(b).

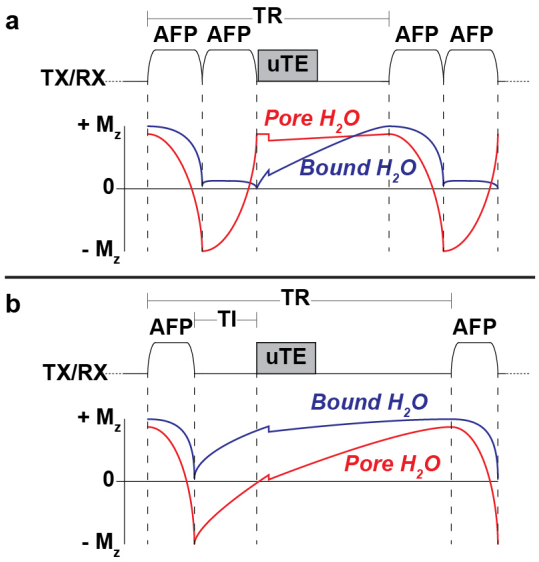

Figure 2: Raw images (top) and quantified bound/ pore water maps (bottom) for DAFP(a) and AIR(b).